CHEMICAL ENGINEERING TRANSACTIONS
VOL. 69, 2018
A publication of AIDIC
The Italian Association of Chemical Engineering
Online at www.aidic.it/cet
Guest Editors: Elisabetta Brunazzi, Eva Sorensen

ISBN 978-88-95608-66-2; **ISSN** 2283-9216

Reaction Enthalpy Conversion in Amine Based Post-Combustion CO_2 Capture

Kangkang Li[a], Paul H.M. Feron[a,*], Kaiqi Jiang[a], Timothy W. Jones[a], Robert D. Bennett[b], Anthony F. Hollenkamp[b], Pauline Pearson[b]

[a]CSIRO Energy, PO Box 330, Newcastle, NSW 2300, Australia
[b]CSIRO Energy, Private Bag 10, Clayton South, VIC 3169, Australia
paul.feron@csiro.au

Aqueous amine based CO_2 capture processes are the the leading technology for the CO_2 emission reduction from the fossil fuel combusted power stations, but its commercial-scale application is largely limited by the intensive energy consumption associated with the capture process. While the CO_2 absorption heat is identified the largest exergy destruction, the present study proposed a metal mediated electrochemical process to harvest the CO_2 absorption enthalpy into electric power to compensate the capture energy consumption. Ammonia as the promising absorbent for CO_2 capture was used to explore the energy conversion performance. The effect of metal types, ammonia concentrations, supporting electrolyte concentrations on the power density performance was investigated. The battery discharge performance was carried out by connecting the external load to the battery. The energy output of 4.1 kJ/mol CO_2 was achieved experimentally at studied conditions, resulting in an enthalpy-to-electricity conversion efficiency of 6.4%.

1. Introduction

Amine-based processes are the leading technology for CO_2 capture from power plant flue gases and other carbonated exhaust gases. While the first large scale commercial applications of this technology have now emerged (the Boundary Dam project in Canada and the Petranova project in Texas), a considerable challenge remains to reduce the energy consumption of the CO_2 capture and compression process to low levels. It is generally considered that a likely lowest overall energy consumption of an optimised, practical post-combustion CO_2 capture process (PCC) will be double the thermodynamic minimum energy requirement (Rochelle, 2009). This is based on the typical thermodynamic performance of industrial separation processes in the chemical industry. For CO_2 capture from a coal fired power station this results in a lowest value of 0.2 MWh/ton CO_2 (Feron, 2011). At present the energy consumption for a state-of-the-art advanced amine processes is estimated at 0.3 MWh/ton CO_2, which is 25% improvement compared to a standard mono-ethanolamine based process (~0.4 MWh/ton CO_2) (Rubin et al., 2015). Technological advances by the technology suppliers have focused on a mix of amine development and process development, for example,

- Maximisation of CO_2 uptake by advanced amine absorbent formulations and absorber intercooling strategies
- Minimisation of reboiler duty through the use of same advanced amines and heat integration methodologies in the desorber.

Significant progress has been made, but further improvements are deemed necessary to lower barriers for technology deployment. Exergy analysis of the amine-based CO_2 capture process has revealed that the CO_2-absorption process a major source for exergy destruction (Geuzebroek et al., 2004). This stems from the fact that the CO_2-absorption process is exothermic, with the energy it produces being dissipated as heat in the absorber. In fact the exothermic character of the absorption process increases the temperature in the absorber, which reduces the driving force. This is obviously undesired and intercooling is common applied, particularly in the advanced processes, which have lower absorbent flow rates, resulting in large temperature excursions in the absorber. Ironically, while the energy released during the absorption process remains

unutilised, it will need to be applied in the desorption process. The focus of all vendor technology developments is on reducing the reboiler duty, but none consider the opportunity for recovery of the absorption enthalpy in a useful manner. Heat recovery from the absorber is possible but the temperature levels at which the heat can be reuse are impractical in terms of reuse.
An alternative energy recovery route is provided by the ligand capabilities of many amines. It is well known that amines including ammonia are able to form complexes with many metals, dissolving them into the solution. These complexes can be reversed by the introduction of carbon dioxide into the solution, which results in the deposition of the metal. This process forms the basis for an electrochemical cell, which is operated by the lean solution and rich solution, converting the absorption enthalpy into power as shown in Figure 1.

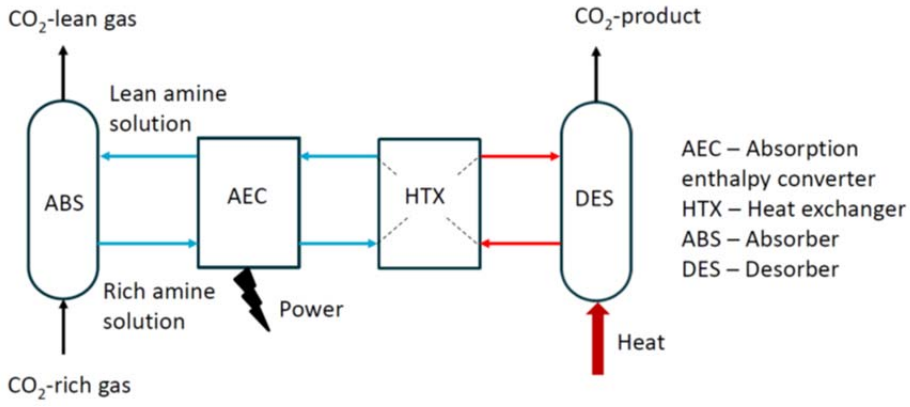

Figure 1: The Absorption Enthalpy Converter in a CO_2-capture process.

The principle for the Absorption Enthalpy Converter is explained by the electrochemical reactions for the aqueous copper-ammine example system. In the anode compartment Cu is dissolved by ammonia:

$$Cu(s) + 4NH_3 \rightarrow [Cu(NH_3)_4]^{2+} + 2e \qquad E^0=-0.04\ V \qquad (R1)$$

Addition of CO_2 directly from a flue gas subsequently releases part of the free Cu-ion.

$$2CO_2 + [Cu(NH_3)_4]^{2+} \rightarrow 2NH_4^+ + 2NH_2COO^- + Cu^{2+} \qquad (R2)$$

The solution is then carried to the cathode where Cu is deposited. In the cathode compartment:

$$Cu^{2+} + 2e \rightarrow Cu(s) \qquad E^0=0.34\ V \qquad (R3)$$

After deposition of Cu on the cathode, the aqueous mixture containing the carbamate and ammonium ion can be thermally regenerated in the usual manner. CO_2 is released from the solution and the recovered ammonia is reused for Cu-dissolution in the anode compartment.
The overall reaction stoichiometry involves 2 mole of CO_2 per mole of Cu being dissolved or deposited. A preliminary assessment based on the voltage difference (0.38 V) results in 73.3 kJ/mol Cu or 36.7 kJ/mol CO_2. At an energy conversion efficiency of 0.75 it would be theoretical to generate 0.62 MJ/kg CO_2 (0.17 kWh/kg CO_2). Compared to standard overall energy requirement of a post-combustion CO_2 capture process (0.4 kWh/kg CO_2), this represents a significant amount of energy and could go a long way towards bringing the energy consumption for CO_2 capture towards the thermodynamic minimum if not zero.
While the process concept is able to utilise a range of amines, the focus here will be in the use of aqueous ammonia as the most robust amine available. This robustness has made it of interest for applications in post-combustion CO_2-capture (Yang, et al., 2014) with GE, formerly Alstom, being the main technology supplier (Augustsson et al., 2017) through its Chilled Ammonia Process (CAP).

2. Methodology

The chemicals of ammonia (NH_3), copper nitrate ($CuNO_3$), nickel nitrate ($NiNO_3$), zinc nitrate ($ZnNO_3$), ammonia nitrate (NH_4NO_3) and ammonia bicarbonate (NH_4HCO_3) were purchased from Sigma Aldrich in analytical grade and used without further purification. Deionised water was used to prepare solutions with

different metals, different NH_3 concentrations and different supporting electrolyte concentrations. The CO_2 loaded ammonia solution was prepared by mixing of NH_3 and NH_4HCO_3. The solution's CO_2 loading was determined in a titration method by measuring the volume of gaseous CO_2 that was liberated by excess nitric acid (HNO_3). The CO_2 volume was measured at atmospheric pressure using two burettes and the CO_2 amount was calculated using the ideal gas law. This method was validated by using the $CaCO_3$ solid with an average error ±3%. The CO_2 loading was determined by three measurements and the average value was used. A static electrochemical cell was designed with a distance of 1.2cm between anode and cathode electrodes, separated by an anion exchange membrane (AEM, Selemion AMV, Japan) as shown in Figure 2. A potentiostat (Autolab PGSTAT12, Metrohm) was used to measure the electrode potentials and power output at different values of the applied current. Metal sponge was used as electrode material for its large surface area. The power density was calculated based on the surface area of immersed membrane. The Ag/AgCl reference electrodes (199 mv versus Standard Hydrogen Electrode, Pine Research) was used to monitor the electrode potentials for anode and cathode by connecting the multimeters (Keithley 2100) with the built-in data acquisition system. Battery discharge was performed in the compact cell with 1.5 ml in each anode and cathode compartment, and it was operated with a fixed 10 ±0.1Ω external resistor with the voltage monitored and recorded by multimeters at every 2 seconds until cell voltage was below 15 mV. The total energy of battery discharging was obtained by integrating the power *vs* time ($W_e = \int UIt$) where *U* is the battery voltage (V), *I* the current (A) and *t* is the time (s). Solution conductivity was measured by LCR meter (GW INSTEK LCR-821) at 100 kHz.

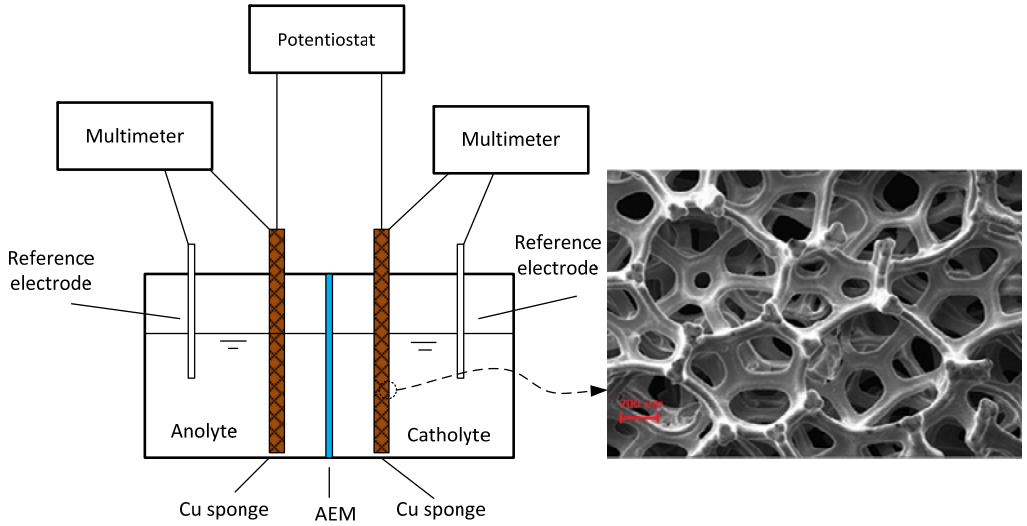

Figure 2 Schematic of experiment set-up in the electrochemical measurement and the Scanning Electron Microscope (SEM) of Cu sponge electrode (X=50)

3. Selection of suitable metals for use with aqueous ammonia

Figure 3 shows the effect of different metals on the power density and electrode potentials of NH_3 based battery. Among the three studied metals, nickel (Ni) had the lowest power density because of the limited potential difference (open circuit potential (OCP) of 0.03V). The poor voltage and battery performance were likely attributed to the Ni-NH_3 complexation in which one mole Ni coordinates six moles NH_3. This makes it more difficult for the complexes to release free Ni^{2+} for metal electrodeposition compared to the copper (Cu) and Zinc (Zn) which usually complex four mole NH_3 ligands. This suggests that the NH_3 based battery system prefers the metal which has less coordination number of ligand. Zn had the best power performance (2.6 W/m^2) owing to its excellent cell voltage (OCP of 0.15 V) and fast redox kinetics. It is anticipated that the complexation ability (lgK=9.46) of Zn-NH_3 is weaker than that of Cu-NH_3 (lgK=13.32), which facilitated the release of free metal ions via the de-complexation by CO_2 absorption and subsequently a better cathode rate capability. However, in the studied aqueous NH_3 system Zn has a very negative reduction potential in the absence (-0.97V) and presence of CO_2 (-0.82V). The NH_3 based CO_2 capture process is usually operated in the pH range of 8-12 during which the reduction potential of hydrogen evolution is 0.48-0.71 V. This indicates that the side reaction of hydrogen evolution is likely to take place in Zn-NH_3 based battery system. Moreover, the Zn electrode is subject to corrosion issue as a result of the oxygen present in the air or the solution due to

its very negative reduction potential. For the sake of experimental feasibility, Cu is therefore preferred as starting material. It has a moderate OCP (0.12V) and power performance (1.4 W/m^2) and excellent redox stability to avoid the hydrogen evolution in aqueous NH_3 solution. It is worthwhile mentioning that the OCP in Cu-NH_3 battery is only one third of the value of 0.38 V as predicted in section 1. This is because CO_2 is a weak acid and its addition into NH_3 solution cannot completely release the free Cu^{2+} from the Cu-NH_3 complexes, resulting in a lower performance of cathode potential.

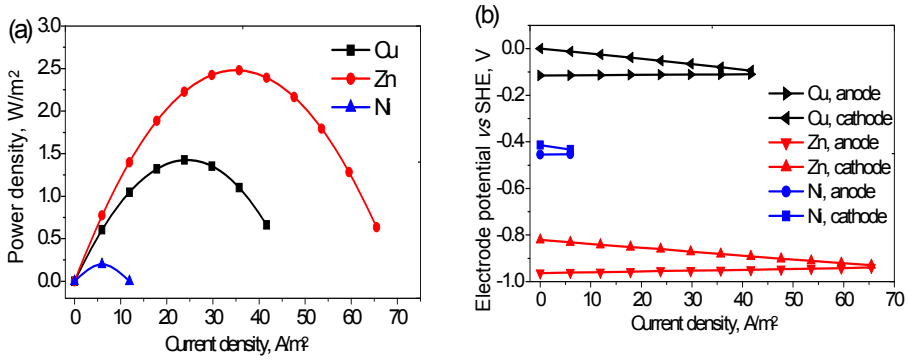

Figure 3 (a) power density and (b) electrode potentials at different metal type, using 2M NH_3, 0.1M metal ions and 1M NH_4NO_3 as supporting electrolyte at 19 °C. The anodic and cathodic solution are without and with ~0.5 CO_2 loading. Note: For Cu and Ni sponge electrodes were used, for Zn plate electrodes were employed to determine the battery performance.

4. Experimental power density performance

Figure 4 shows the power performance of NH_3 battery and the electrode potentials over a range of ammonia concentration using 1M NH_4NO_3 supporting electrolyte. It is observed from Figure 4(b) that both electrode potentials for anode and cathode were decreased due to the increased NH_3 concentration. This can be easily explained by the Nernst equation corresponding to reaction (R1):

$$\mathrm{E} = E^o + \frac{RT}{2F}\ln\frac{[Cu(NH_3)_4^{2+}]}{[NH_3]^4} \qquad \text{(E1)}$$

Where E^o is the standard potential of $[Cu(NH_3)_4^{2+}]/Cu_{(s)}$, -0.04 V; F is the Faraday constant, 96485 C/mol; R is gas constant, 8.314 J·mol^{-1}·K^{-1}; T is the absolute temperature, K. The $[Cu(NH_3)_4^{2+}]$ concentration at different NH_3 concentration was similar due to the fact that the $Cu(NH_3)_4^{2+}$ was the dominant complex species at the studied CO_2 concentration and [Cu] concentration was fixed at 0.1 M. As such an increase of NH_3 concentration reduced the Cu electrode potentials. However the decrease for anode and cathode electrodes were similar, leading to the stabilized OCP at ~0.12 V in the NH_3 concentration range of 2-8 M. The increased NH_3 concentration greatly reduced the anode potential which favours the anodic copper oxidation, whilst it also appreciably decreased the cathode potential, leading to the difficulty of cupric electrodeposition. This results in a trade-off between improved anode performance and decreased cathode rate capability, leading to a very slight improvement of maximum power density of 1.4 W/m^2 at 2 M to 1.5 W/m^2 at 6 M (Figure 4a). The slight increase of power performance is most likely due to the increase of solution conductivity as a result of CO_2 absorption which generated more ionic species at higher NH_3 concentration. This is evidenced by the decrease of solution resistance (Rs) from 6.9 Ω at 2M to 6.2 Ω at 6M NH_3.

It is worth noting that with the increased current density, the anode potentials are slightly affected owing to the large anode rate capability, but the cathode potentials underwent a quick drop, particularly in the high NH_3 concentration (Figure 4b). This means that cathode electrodeposition rate capability is the rate-controlling reaction which determined the maximum power performance. This is particularly obvious at high current density where larger cathode over-potentials and lower power density were observed at 6M and 8 M NH_3 concentration. Moreover, high NH_3 concentration tends to have the issue of precipitation at low temperatures and it is also not preferred due to the NH_3 slip problem during the CO_2 capture process. Therefore NH_3 concentrations below 6 M is suggested,

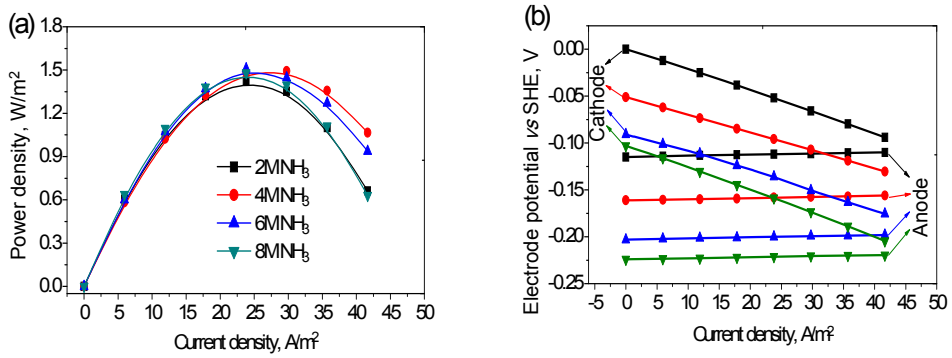

Figure 4 (a) power density and (b) electrode potentials as a function of current density at various ammonia concentration, using 1M NH_4NO_3 as supporting electrolyte at 19 °C. The anodic and cathodic solution are 0 and ~0.48 moleCO_2 /mole NH_3 loading, and each compartment contains 0.1 M $Cu(NO_3)_2$.

The effect of NH_4NO_3 concentration as supporting electrolyte on the power performance was investigated. As shown in Figure 5, the increase of NH_4NO_3 concentration from 1M to 3M improved the power density from 1.5 W/m^2 to 2.3 W/m^2, due to the decreasing solution resistance from 6.2 Ω to 5.4 Ω. However, a further increase in NH_4NO_3 concentration showed the negative effect on the power performance. This is because of the NH_4NO_3 property as a weak acid salt, which decreased the basicity of the NH_3 solution. As shown in the inserted table in Figure 5 (b), the solution pH of both anolyte and catholyte decreased with the increasing NH_4NO_3 concentration. This weakened the capability of CO_2 absorption leading to a lower CO_2 loading of catholyte. As a result, the battery voltage and power performance was reduced as the NH_4NO_3 concentration over 3 M. Moreover, precipitation was observed in the solution of 5M NH_4NO_3 and a worse solid formation occurred in the solution of 7M NH_4NO_3 concentration. This also accounted for the slight drop in power density in 5M NH_4NO_3, and large drop in 7 M NH_4NO_3 compared to the 3M NH_4NO_3 concentration.

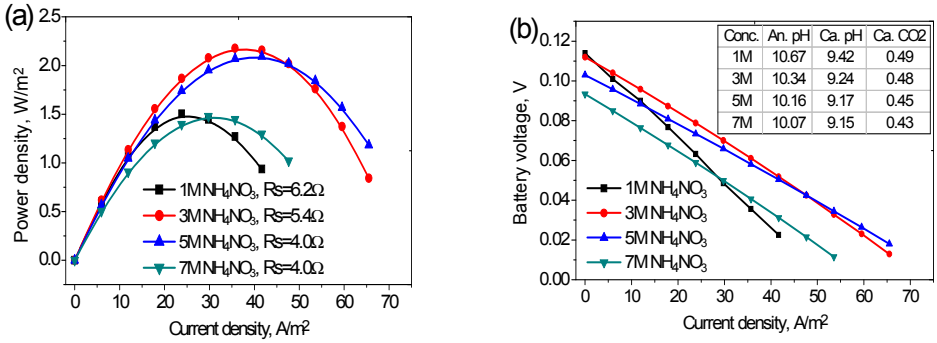

Conc.	An. pH	Ca. pH	Ca. CO2
1M	10.67	9.42	0.49
3M	10.34	9.24	0.48
5M	10.16	9.17	0.45
7M	10.07	9.15	0.43

Figure 5 (a) power density and (b) cell voltage at various NH_4NO_3 concentration at 19 °C. The anodic and cathodic solution are without and with CO_2 loading, and each contains 0.1 M $Cu(NO_3)_2$. The inserted table is the pH values at different NH_4NO_3 concentration. The inserted table shows the pH values of anolyte and catholyte, and the CO_2 loading of cathode solution.

5. Battery discharging performance

Figure 6 shows the voltage changes over an external load as a function of time during the battery discharge. To achieve the practical CO_2 capture process and better battery performance, the CO_2 loading (the ratio of mole CO_2 to mole NH_3) for anode and cathode solutions was determined as 0.06 and 0.44 respectively between which the CO_2 absorption and desorption is performed. The [Cu] concentration of anolyte and catholyte was determined as 0.1 M and 0.35 M respectively. This means that [Cu] in the anolyte increases from 0.1M to 0.35 M whilst [Cu] concentration in the catholyte decreases from 0.35 M to 0.1M, thus achieving the metal material balance in the electrochemical process. Whereas the aforementioned anolyte/catholyte compositions were used for a preliminary assessment of energy discharge performance from the Cu-NH_3 battery, further optimisation studies will most likely result in better anolyte/catholyte compositions. Two parallel experimental battery discharging was performed with the starting voltage of ~0.25V. The higher voltage was

attributed to the improved performance of cathode potentials as a result of increased [Cu] concentration indicated by E1. With the battery discharge, the load voltage decreased which converted the chemical energy into electric power. The load voltage dropped quickly in the first 30 minutes and then decreased slowly. This is because the electroactive species for redox reactions are abundant at the beginning of battery discharge and depleted with time going. By integrating the load voltage as a function of time, the experimentally achieved energy was calculated about 4.1 kJ/mol CO_2. Our previous study has indicated that the reaction enthalpy of CO_2 by aqueous NH_3 was approximately 66 kJ/mol CO_2 (Li et al., 2015). This resulted in the enthalpy-to-electricity conversion efficiency of 6.4% at studied conditions.

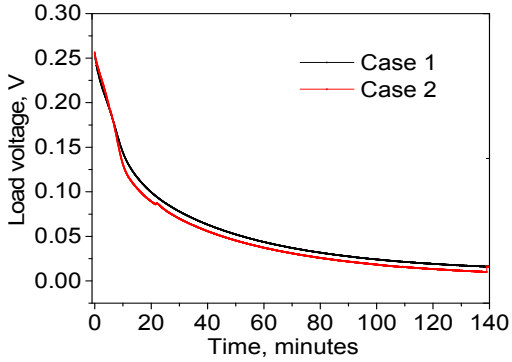

Figure 6 Energy performances of the Cu-NH_3 based battery using 2 M NH_3, 3 M NH_4NO_3 as supporting electrolyte at room temperature (19 ^oC). Cu concentrations are 0.35 M in catholyte and 0.1M in anolyte. The CO_2 loadings are 0.44 in catholyte and 0.06 in anolyte. An external resistance of 10 Ω was used during the battery discharging.

6. Conclusions

The present study has demonstrated the effectiveness of the conversion of CO_2 reaction enthalpy into electric power in aqueous NH_3 based CO_2 capture process. Cu was identified as the preferred starting metal for the enthalpy conversion process. Increasing the NH_3 concentration from 2M to 8 M had little influence on the power density performance, and a 3 M NH_4NO_3 concentration as supporting electrolyte resulted in the best power performance. The battery discharge experiments showed an energy output of 4.1 kJ/mol CO_2, resulting in the enthalpy-to-electricity conversion efficiency of 6.4%. Future work will focus on the process optimization to identify the best operation conditions of battery discharge and the extension of NH_3 to other amines for better energy performance.

Acknowledgments

We acknowledge Coal Innovation New South Wales for funding support, and thank Scott McGarry for the 3D printing of the electrochemical cell.

References

Augustsson, O., Baburao, B., Dube, S., Bedell S., Strunz, P., Balfe, M., Stallmann O., 2017, Chilled Ammonia Process Scale-up and Lessons Learned, Energy Procedia, 114, 5593-5615

Feron, Paul H.M., 2010, Exploring the potential for improvement of the energy performance of coal fired power stations with post-combustion capture of carbon dioxide, International Journal of Greenhouse Gas Control 4, 152–160

Geuzebroek, F.H., Schneiders, L.H.M.J., Kraaijveld, G.J.C., Feron, P.H.M., 2014 Exergy analysis of an alkanolamine-based CO2 removal unit with AspenPlus, Energy, 29, 1241-1248

Rochelle, G. T. 2009, Amine scrubbing for CO_2 capture. *Science* 325, 1652-1654

Rubin, E. S., Davison, J. E. & Herzog, H. J., 2015, The cost of CO_2 capture and storage. International Journal of Greenhouse Gas Control 40, 378-400

Yang, N., Yu, H., Li, L., Xu, D., Han, W., Feron P., 2014, Aqueous Ammonia (NH_3) Based Post Combustion CO2 Capture: A Review, Oil & Gas Science and Technology – Rev. IFP Energies Nouvelles, 69, 931-9

Li, K.; Yu, H.; Feron, P.; Tade, M.; Wardhaugh, L. Technical and energy performance of an advanced, aqueous ammonia-based CO2 capture technology for a 500 MW coal-fired power station. Environ. Sci. Technol. 2015, 49, 10243−10252.